Journal of Catalysis **188,** 14–23 (1999)
Article ID jcat.1999.2657, available online at http://www.idealibrary.com on IDEAL®

Preparation and Characterization of MCM-41 Supported Metallocene Catalysts for Olefin Polymerization

Hanna Rahiala,*[,1] Isabelle Beurroies,* Tom Eklund,* Kimmo Hakala,† Regis Gougeon,‡
Philippe Trens,§ and Jarl B. Rosenholm*

*Department of Physical Chemistry, Åbo Akademi University, Porthansgatan 3-5, FIN-20500 Åbo, Finland; †Polymer Science Centre,
Helsinki University of Technology, P.O. Box 356, FIN-02151 Espoo, Finland; ‡Department of Chemistry, University of Durham,
South Road, Durham, GB-DH1 3LE, Great Britain; and §Department of Chemistry, University of Reading,
Box 224, Whiteknights, Reading GB-RG6 6AD, Great Britain

Received November 16, 1998; revised July 19, 1999; accepted August 4, 1999

The effect of the structure and surface properties of support material on metallocene (zirconocene chloride) adsorption and catalyst activity in ethene polymerization was studied. Commercial Grace silica, mesoporous silicate, MCM-41, and aluminium-modified MCM-41 were used as supports. The highest amount of zirconocene dichloride was adsorbed on Al-modified MCM-41 (Si/Al = 32), providing the most reactive sites for attachment of the active component on the support surface. The ^{13}C-CPMAS NMR studies proved that Cp_2ZrCl_2 is bound to the support surface. Also the highest activity in ethene polymerization was obtained using this support.
© 1999 Academic Press

Key Words: **mesoporous silicate; MCM-41; heterogeneous catalysis; metallocene; olefin polymerization.**

INTRODUCTION

Metallocene catalysis can be considered as a major breakthrough in polyolefin technology (1–4). Several studies reported in the literature (5–10) have concentrated on the use of supported metallocene complexes in the olefin polymerization. Silica, alumina, and magnesium compounds are the most used inorganic supports (2, 11). By heterogenization the morphological characteristics of the polymers and the metallocene activation step are improved (12). The aim is to find a way to attach the metallocene to the support without losing the performance of the homogeneous complex. Three main immobilization techniques can be classified, direct impregnation of metallocenes on the support, pretreatment of the support with ordinary alkylaluminiums or methylaluminoxane (MAO) followed by the reaction with the metallocene compound, and immobilization of metallocene ligands on the supports followed by addition of transition metal salts (10).

The main problems still faced in heterogenization are lower yields and catalyst activity as compared to homogeneous system (5–10). Furthermore, a need of a threshold level of MAO to work (Al/Zr range of 50–400) (12, 13) and desorption of the metallocene from the catalyst when using methylaluminoxane (MAO) as a cocatalyst (14) are serious drawbacks. However, high molecular weights and melting temperatures, narrow molecular weight distributions, and improved polymer properties have been achieved for supported catalysts (4, 12, 15). The reasons for the low catalyst activities are not clear, but the steric hindrance around the active site on the silica surface seems to be one constraint (16). The introduction of a spacer molecule such as trisiloxane or pentamethylene (16) or silanes (17) between metallocene and silica has resulted in increased catalyst activity in ethene polymerization. Also, high surface area and the presence of well-defined, stable sites for the attachment of the active component to the support have been found to be of importance (15). Mesoporous silicate, MCM-41, is a member of a new family of mesoporous molecular sieves, M41S, invented by Mobil researchers in 1992 (18, 19). The regular, cylindrical and hexagonally ordered pores of MCM-41 have been observed to suppress the formation of inactive binuclear complexes between two metallocenes or between metallocene and methylaluminoxane, resulting in stable active sites and high activity in propene polymerization (20–22). The pores are large (2–10 nm, depending on the alkyl chain length of surfactant) compared to, e.g., zeolites, which could enable large metallocene molecules to be witheld not only on the surface but also inside the supercage of the support.

In the present study the effect of structural features of the Grace silica and MCM-41 supports on the metallocene catalyst activity in ethene polymerization was evaluated. In accordance with recent publications (23, 24) indicating that the incorporation of other elements into the silicate framework enhances the catalytic activity in different reactions, the MCM-41 was modified with low concentrations of

---

[1] To whom correspondence should be addressed, the Graduate School of Materials Research, Åbo, Finland. Fax: 358(0)2 215 4706. E-mail: hrahiala@abo.fi.

0021-9517/99 $30.00

aluminium. The effect of aluminium on the structure and surface properties of MCM-41 and further on the adsorption of the metallocene, zirconocene dichloride, on the support surface and on the catalyst activity was investigated. The location and coordination states of aluminium after calcination were of interest since aluminium is the origin of the Brønsted acidity of aluminosilicate (25).

EXPERIMENTAL

Synthesis

The commercial silica (Grace, S8MY) was heat-treated at 420°C for 20 h before use, which is expected to leave around 4 OH/nm^2 (26). The Si-MCM-41 was synthesized at 30°C using hexadecyltrimethylammonium bromide (C_{16} surfactant, HTABr, Aldrich), water, NH_3 (32% extra-pure, Merck), and tetraethyl orthosilicate (TEOS, 98%, Aldrich) as starting materials. The surfactant (0.048 M) was first dissolved in water at 30°C, followed by addition of ammonia (1.03 M) and TEOS (0.325 M). The white precipitate was filtrated after 1 h of mixing, washed, dried at 90°C (24 h), and calcined at 550°C (5 h; 1°C/min). The heat treatment removes the template molecules (surfactant) and gives around 3 OH groups/nm^2 on the MCM-41 surface (27). Additional aluminium (molar ratio of Si/Al = 150, 100, 50, 20, and 5) was incorporated into the MCM-41 framework during synthesis using aluminium isopropoxide (Aldrich, 99.99+%) as a metal source. Aluminium isopropoxide was dissolved in 1-propanol (Merck, >99.5%) before use.

Catalyst Preparation

The metallocene, zirconocene dichloride (Cp_2ZrCl_2, Aldrich, Cp = cyclopentadienyl), was immobilized on commercial silica (Grace, S8MY), MCM-41, and Al-modified MCM-41 (Si/Al = 20). The immobilization was carried out in toluene (J. T. Baker, >99.5%; dried using Na metal and benzophenone (Merck, >99%)) under nitrogen atmosphere. Certain amounts of zirconocene dichloride were adsorbed on the dehydrated supports to obtain zirconium contents of 3.1 wt% (Grace SiO_2, RT), 2.7 wt% (Grace SiO_2, 70°C), 4.7 wt% (MCM-41, RT), and 4.8 wt% (Si/Al = 20, RT). After the reaction, the solid part was washed with toluene and dried in vacuum.

Method of Polymerization

The reactor (0.5 dm^3) was evacuated and flushed with nitrogen several times before we added toluene (Merck, GR grade), MAO solution (10 wt% in toluene, Witco), and the catalyst suspension in toluene (300 ml). The polymerization reaction was started by introducing the ethylene (Air Liquide, Grade 3.5) flow. Polymerization temperature (50°C) and partial pressure of ethylene (2.5 bar) were kept constant during reaction. The polymerization was stopped after 30 or 60 min, and the polymer was precipitated with dilute HCl solution in ethanol, filtered, washed with ethanol, and dried in vacuum. Methylaluminoxane, MAO, was used as a cocatalyst with the Al/Zr molar ratio of 2000. The blank reaction was done under the same conditions using only MAO for the reaction.

Characterization of Supports and Catalysts

X-ray powder diffraction (PHILIPS PW 3710; Cu$K\alpha$ radiation) and thermoporometry (28, 29) (GETARAM DSC 92; He atmosphere; water as solvent) were used to verify the pore structure and to determine the pore radius (r) of the calcined (550°C) MCM-41 supports. The nitrogen adsorption/desorption isotherms, the BET (Brunauer, Emmett, and Teller) surface area, and the pore size distribution (Barrett–Joyner–Halenda (BJH) formula (30, 31)) for supports and catalysts were measured using Micromeritics ASAP 2010 equipment. Prior to the analyses, the samples were pretreated at 150°C (support) or at 70°C (catalyst).

The silicon, aluminium, and zirconium metal contents were determined using ICP-MS. The thermogravimetric (Netzsch TG-209) analyses of the dried samples were carried out in air to simulate the calcination process in the oven during sample preparation (2 h at 90°C, 90–550°C 1°C/min, 5 h at 550°C). The solid-state ^{27}Al-NMR spectra (background subtracted) were measured using a Varian Unity Plus 300 spectrometer (78.156 MHz, a high-speed MAS probe from Doty Scientific) with direct polarization, 0.6 μs pulse duration (15° pulse angle), 8700 Hz spinning speed, and 0.5 s recycle delay. The chemical shifts were referenced to a saturated $AlCl_3$ solution.

The solid-state ^{1}H-MAS-NMR (a Chemagnetics CMX infinity 400 MHz spectrometer) experiments were carried out using 11.3 kHz rotation, 64 transients, 2.5-μs pulse, and 20-s delay time. The samples were pretreated under vacuum for 2.5 h at 400°C. The FTIR (Bruker IFS 66) spectra were recorded using a diffuse reflectance unit (DRIFT) and potassium bromide as background material. The resolution of the FTIR equipment was 4 cm^{-1}. The pore structure of the support materials was evaluated with transmission electron microscopy, TEM (Philips CM20, used with a high tension of 200 kV). The samples were deposited from a slurry in ethanol on Cu/carbon lacey grids (AGAR).

The solid-state ^{13}C-CPMAS NMR experiments (Chemagnetics CMX 270 Infinity NMR spectrometer) of catalysts were performed using the parameters 4.5-μs (90°) pulse (55 kHz r.f. fields), 2.0-ms contact time, 5.0-s recycle delay, 15000 (Grace) or 50000 (MCM-41) transients, and 5.0 kHz MAS rotation frequency.

The molecular weights and molecular weight distributions of polyethenes (PE) were determined with a Waters 150C gel permeation chromatograph (GPC) operating at 140°C from samples dissolved in 1,2,4-trichlorobenzene.

The melting temperatures (T_m) of polymers were measured with a Mettler Toledo Star DSC821 differential scanning calorimeter (DSC) upon reheating of the polymer sample to 150°C at a heating rate of 10°C/min.

RESULTS AND DISCUSSION

Support

Structural features of Grace silica and MCM-41. The morphologies of the commercial silica (Grace, S8MY) and MCM-41 are clearly different. Grace silica consists of particle aggregates with an average size of 70 μm while the main structural feature of MCM-41 is the pore structure not between, but inside the particles. The thickness of the silicate walls is around 1 nm (18). Both materials are amorphous, but the hexagonally ordered pores of the MCM-41 give rise to XRD reflections which are typical for hexagonally ordered mesoporous materials (Fig. 1) (18). The characteristic Bragg peaks with *d*-spacings 3.88, 2.25, 1.97, and 1.47 nm correspond to reflections from the (100), (110), (200), and (210) planes, respectively.

The pore shape, pore size, pore size distribution, and pore connectivity are the most important factors for the adsorption reaction between the active component and the support (11). The N_2 adsorption/desorption isotherms and pore size distributions in Fig. 2 show clearly the difference between these two materials. The large pores between the particles filled at high relative pressures and broad pore size distribution (6–30 nm) are characteristic for Grace silica. The inflection in the adsorption isotherm of MCM-41 reflects the filling of the mesopore system. The pore size distribution is narrow (2–3 nm), as seen in Fig. 2b. BET surface areas of 372 and 1093 m^2/g and pore volumes of 1.7 and 1.03 ml/g were observed for Grace silica and MCM-41, respectively. The pores with small and regular size in MCM-41 are expected to provide space and stable active sites for metallocene adsorption and to prevent the formation of a complex between two metallocene molecules (20, 21). For Grace silica supported metallocene catalyst the formation of binuclear complexes has been observed, resulting in inactive sites after immobilization (20, 21).

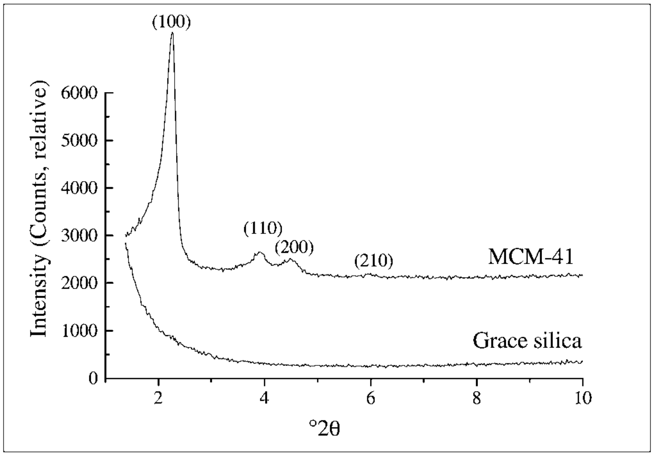

FIG. 1. The X-ray powder diffration patterns for Grace silica and Si-MCM-41.

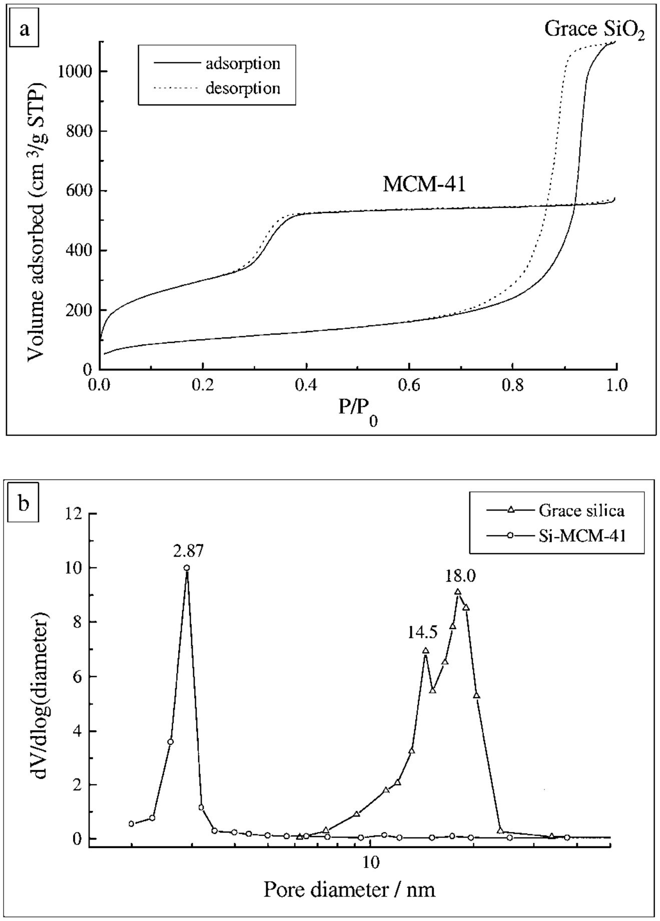

FIG. 2. The nitrogen adsorption/desorption (a) and pore size distribution (b) curves for Grace silica and Si-MCM-41.

Effect of Al-incorporation on the MCM-41 structure. The results of elemental analysis, X-ray powder diffraction, thermoporometry, and N_2 adsorption/desorption studies of the MCM-41 supports (550°C) are collected in Table 1. The modified samples contain 0.5–6.2 wt% aluminium. The mass balance yield of Al-incorporation (exp/theor) is 97–44% with increasing aluminium concentration. The lower Al contents obtained in the final product (Si/Al = 152, 116, 60, 32, and 10) compared to the initial amounts (Si/Al = 144, 100, 50, 20, and 5) are most probably due to imperfect dissolution of Al-alkoxide in 1-propanol.

The thermogravimetric analysis of the dried samples (90°C) showed that water and organics are released or burned from the structure in three main steps (Fig. 3), at 90–205, 205–265, and 265–350°C. The steps relate to

TABLE 1

The Results of Elemental Analysis, X-Ray Powder Diffraction, Thermoporometry, and N_2 Adsorption/Desorption Studies of the Prepared Supports

Support	Si/Al, initial (molar ratio)	Metal content (wt%)	Si/Al, final (molar ratio)	BET surface area (m^2/g)	Pore volume (cm^3/g)	Average pore diameter[a] (nm)	Pore radius[b] (nm)	Pore radius[c] (nm)	*d*-value, XRD (nm)
Grace SiO_2				372	1.7	6-30			
Si-MCM-41		Si 45.68		1093	1.0	2.9	1.50	1.92	3.88
Si/Al = 150	144	Si 43.81 Al 0.47	152	1138	0.99	3.1	1.54	1.94	4.02
Si/Al = 100	100	Si 48.51 Al 0.68	116	1131	0.99	3.1	1.52	1.92	3.97
Si/Al = 50	50	Si 46.16 Al 1.25	60	1099	0.95	3.1	1.54	1.94	4.11
Si/Al = 20	20	Si 46.97 Al 2.42	32	1126	0.99	2.8	1.45	1.87	3.88
Si/Al = 5	5	Si 39.46 Al 6.19	10	1020	0.50				

[a] The values were determined using the desorption branch of the N_2 isotherm and the BJH formula (30, 31).

[b] The values were determined by thermoporometry using the equation $1/d = ((1/T) - (1/T_0))/(1/401.65)$, where T_0 is 276.17 K (37).

[c] The values were determined by thermoporometry using the equation $r = (-64.67/(-)\text{Peak Top Temp.}) + 0.57$ (38).

removal of water inside the pores and/or the template molecules not involved in the silicate structure, the desorption of the main part of the template molecules involved in the silicate structure, and the combustion of the remaining carbon species (e.g., adsorbed trimethylamine, fractionated template molecules, residual carbon, and deposited carbon), respectively (27). The weight loss at higher temperatures (>350°C) is due to the burning of the rest of the organics and/or the loss of water released as a result of condensation of silanol groups to siloxane bonds (32). The total weight loss is diminished from 43 to 35% with increasing Al content. All the organics are burned off and no dealumination seems to occur during the calcination. According to the literature (32, 33–36), partial dealumination has been observed at higher than 400°C calcination temperatures.

The structural analysis (XRD and TEM) of the Al-modified MCM-41 supports showed that the hexagonal pore structure of MCM-41 becomes less ordered with increasing aluminium concentration (Figs. 4 and 5). Using this particular synthesis route the maximum amount of aluminium that can be incorporated to keep the hexagonal ordering is 2.4 wt%. The TEM image shows still some level of ordering of the pores for Si/Al = 10, but not enough to be detected by XRD. The Si/Al = 32 support is suitable for catalyst preparation and further for polymerization reaction.

A high surface area material was obtained for all samples (Table 1). The main property required for the support, i.e., a high surface area available for the active component, is therefore still fulfilled (11). The pore size was observed to slightly diminish with increasing Al content.

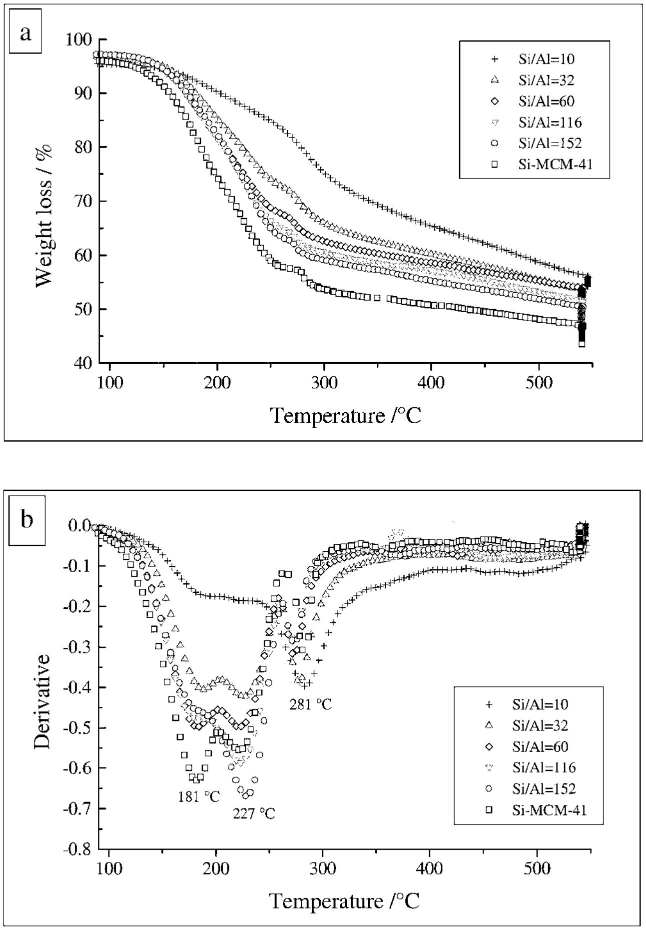

FIG. 3. The TG (a) and DTG (b) curves for MCM-41 supports.

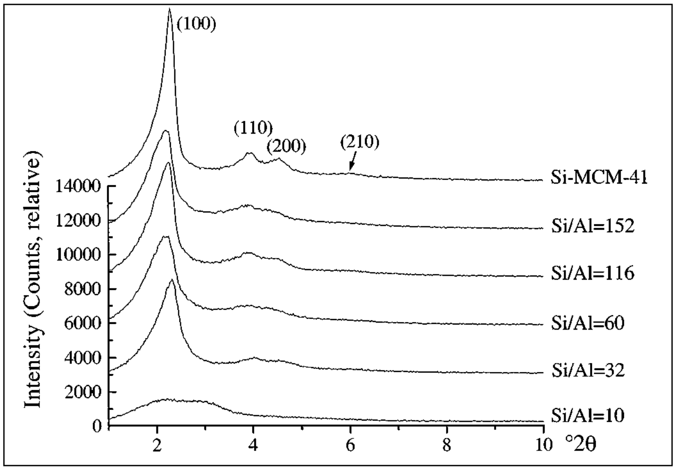

FIG. 4. The X-ray powder diffraction patterns for Si-MCM-41 and Al-modified MCM-41 supports.

The following ranges were obtained for the pore diameter (Table 1): d (sorptometry) = 2.8–3.1 nm, d (thermoporometry, Eq. [1]) = 2.90–3.08 nm, and d (XRD) = 2.88–3.11 nm. The agreement is obviously quite spectacular. The wall thickness (~1 nm) was taken into account in the case of the XRD results, and the freezing temperature of water within the pores determined by thermoporometry was related to the solid–liquid interface curvature using Eqs. [1] and [2] (T_0 is 276.17 K) (37, 38).

$$\frac{1}{d} = \left(\frac{1}{T} - \frac{1}{T_0}\right)\bigg/(1/401.65) \qquad [1]$$

$$r = \frac{-64.67}{(-)\text{Peak Top Temp.}} + 0.57 \qquad [2]$$

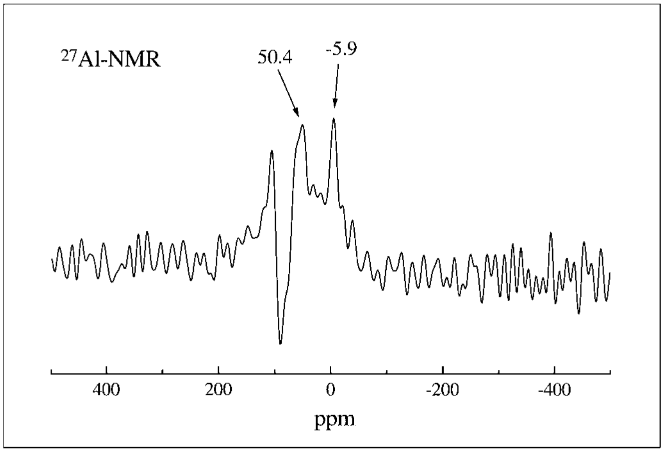

FIG. 6. The solid-state ^{27}Al-NMR spectrum for MCM-41 containing 6.2 wt% of additional aluminium.

State of the incorporated Al and number of the surface sites. The location of aluminium together with the number and type of the surface sites are of importance as the active component is adsorbed on the support. These properties were determined using solid-state ^{27}Al-NMR, ^{1}H-MAS-NMR, and FTIR spectroscopy. The ^{27}Al-NMR spectrum was obtained only for the sample (550°C) containing the most aluminium (6.2 wt%) because of the limited sensitivity of the equipment. The two peaks observed at 50.4 and −5.7 ppm are related to the 4-coordinated and the 6-coordinated aluminium, respectively (Fig. 6) (33). The 4-coordinated aluminium is structural and the 6-coordinated one is most probably located in the pores. The peak at 104.0 ppm is caused by the background. The results are in accordance with the work done by several other research groups (34–36): only less than 3 wt% of aluminium

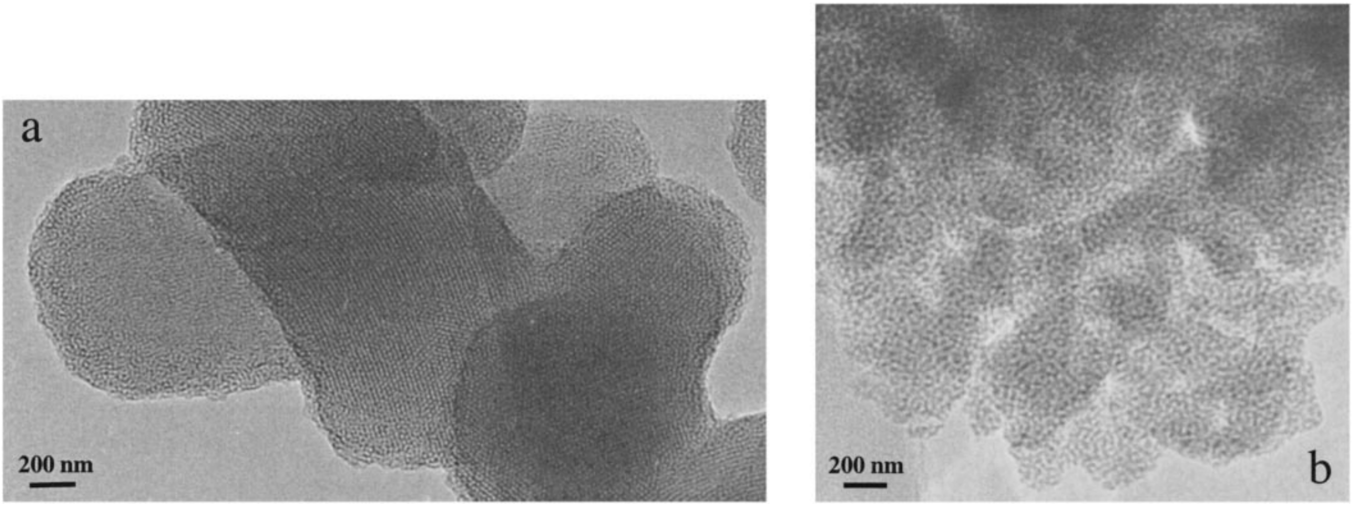

FIG. 5. The TEM images for Si-MCM-41 (a) and Al-modified MCM-41 (Si/Al = 32) (b). The light areas in the images correspond to a lack of scattering matter (pores), and dark areas are concentrations of scattering material (walls). The magnification is 380000× .

have been managed to be incorporated into the silicate framework. The source of silicon and aluminium has been found to be a key factor for the state of incorporation (30, 34–36). Janicke *et al.* (39) have recently shown that octahedral aluminium environments could be formed by strong interactions between framework Al species and adsorbed water or surfactant molecules in the mesoporous channels in the as-synthesized aluminosilicate MCM-41 material. During calcination the octahedral Al sites could be converted into species with tetrahedral coordination. The obtained framework aluminium induces a slightly higher degree of Brønsted acidity for Al-modified MCM-41 (Si/Al = 10) compared to purely siliceous MCM-41.

The densities of OH groups of 19.4 and 16.3×10^{20} OH/g were obtained for MCM-41 and Si/Al = 32 using solid-state ^{1}H-MAS-NMR. These relate to 1.8 and 1.4 OH groups/nm^2. The results indicate that less binding sites/nm^2 are available in the MCM-41 silica than in Grace silica (around 4 OH groups/nm^2) (26). On a mass basis the number of OH groups, 14.9×10^{20} for Grace silica and $19.4–16.3 \times 10^{20}$ for MCM-silica, are nearly equal. A comparison of the total number of OH groups might give a misleading value of the groups available for surface reactions, since some sites remain inaccessible even after high-temperature treatments (40). The number of OH groups obtained for MCM-41 is fewer than the values found in the literature (27) (2.5 to 3 OH/nm^2), but the synthesis route, starting materials, and synthesis conditions have a big influence on the surface properties (41). No evidence for the presence of acidic AlOHSi type OH groups (between 3.5 and 5.0 ppm) could be obtained for the sample Si/Al = 32. The spectrum consisted of one main peak at about 2.0 ppm and a shoulder at 2.4 ppm, due to Si–OH groups, and a broad peak at about 3.5 ppm, due to residual water. This result is in agreement with the ^{27}Al-NMR studies.

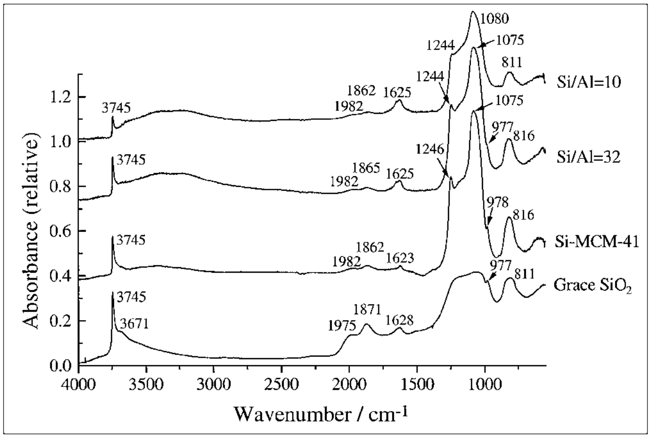

FIG. 7. The FTIR spectra for Grace silica, Si-MCM-41, and Al-modified MCM-41 (Si/Al = 32 and Si/Al = 10).

TABLE 2

The Results of the Zirconium Analysis of the Prepared Catalysts

Support	Zr_0 (wt%)	$Zr_{anal.}$ (wt%)	$Zr_{ads.}$ (%)	$C_{anal.}$ (wt%)	n(C/Zr)
Grace SiO$_2$, RT	3.1	1.1	35.5	1.9	13.2
Grace SiO$_2$, 70°C	2.7	1.2	44.4	2.2	13.5
Si-MCM-41	4.7	1.6	34.0	6.1	28.5
Si/Al = 32	4.8	2.7	56.3	6.3	18.1

The FTIR spectra for Grace silica (420°C), Si-MCM-41 (550°C), and Al-modified MCM-41 (Si/Al = 32 and Si/Al = 10; 550°C) do not show any big differences (Fig. 7). The peaks at 3745 and about 977 cm^{-1} are related to isolated single Si–OH groups. The vibrations caused by siloxane bridges, Si–O–Si, are observed at 1350–910 and about 811 cm^{-1} together with the overtone peaks at 1975 and 1870 cm^{-1}. When aluminium is added to the MCM-41 structure the peak at 3745 cm^{-1} decreases and the peak at 978 cm^{-1} disappears. Also, the peaks due to Si–O–Si vibrations are observed to diminish. It is difficult to detect any Si–O–Al vibrations and additional OH groups as a result of Al incorporation, most probably because of overlapping of peaks due to the low Al-concentration.

Catalyst Characterization

The results of the zirconium analysis of the prepared catalysts are collected in Table 2. The catalysts immobilized on Grace silica (RT and 70°C), Si-MCM-41, and Al-modified MCM-41 (Si/Al = 32) contained 1.1 (RT), 1.2 (70°C), 1.6, and 2.7 wt% zirconium, respectively. The highest amount of added zirconium, 56%, was adsorbed on the Al-containing MCM-41 support. The zirconium adsorption was observed to occur equally on siliceous MCM-41 and on Grace silica supports (∼35%). The higher immobilization temperature (70°C), however, enhanced the Zr adsorption on Grace silica by 9%. Additional aluminium seems to have a big effect on the surface properties of MCM-41, giving more reactive surface sites for Cp_2ZrCl_2 to bond as compared to the purely siliceous MCM-41. The temperature programmed desorption (TPD) studies of ammonia and the adsorption studies carried out using organic probe molecules with different Lewis/Brønsted acidity/basicity support this result (42). The results clearly indicate the increase in number and strength of surface sites as a result of addition of aluminium in the MCM-41 structure.

The ^{13}C-CPMAS NMR spectra (Fig. 8) measured for the Cp_2ZrCl_2-Grace SiO$_2$ and Cp_2ZrCl_2-Si/Al = 32 catalysts show one sharp peak at 115 ppm. The peak is related to the cyclopentadienyl (Cp) ring bonded to zirconium (43), and according to studies of Kröger-Laukkanen *et al.* (44) the species on the surface might be X_3ZrO–Si (where X is Cp or Cl). A shoulder at 117.9 ppm is observed for Si/Al = 32-Cp_2ZrCl_2 catalyst. This might indicate that zirconium is bound to two oxygens, the species being X_2Zr(OSi)$_2$

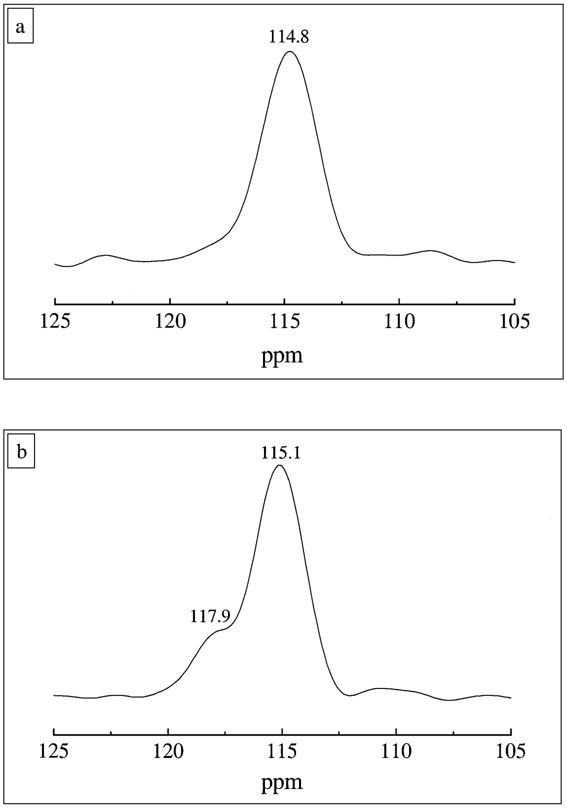

FIG. 8. The ^{13}C-CPMAS NMR spectra for (a) Cp_2ZrCl_2-Grace SiO_2 and (b) Cp_2ZrCl_2-MCM-41-Si/Al = 32 catalysts.

(44). The results prove that the zirconocene is bound to the support surface mainly via isolated OH groups and on Al-modified MCM-41 partly via hydrogen-bonded OH groups. Maschmeier *et al.* (45) have observed titanocene dichloride to mainly anchor on MCM-41 via three oxygen atoms.

The maximum Van der Waals radius of the zirconocene dichloride molecule is 0.79 nm (calculated from the crystal structure (3)). The pores with an average diameter of 2.9 nm (Si-MCM-41) and 2.8 nm (Si/Al = 32) (Table 1) would thereby provide space for one Cp_2ZrCl_2 molecule to bind to the surface OH groups inside the pores. The pore structure and pore size after the immobilization of Cp_2ZrCl_2 onto the MCM-41 and Al-modified MCM-41 supports were studied by X-ray powder diffraction and N_2 adsorption/desorption measurements (Table 3 and Fig. 9). It is important that the pore shape remain ordered and that there is enough space for the chain-transfer to occur after immobilization. The XRD studies showed that the ordered pore structure of the MCM supports is still left after the immobilization (Table 3). The intensity of the (100) peak in the XRD pattern decreased as a result of immobilization. The BET surface area, pore volume, and average pore diameter were observed to decrease, 34 m^2/g/0.05 ml/g/0.08 nm in the case of Si-MCM-41 and 210 m^2/g/0.35 ml/g/0.21 nm for Al-modified MCM (Si/Al = 32), respectively (Table 3, Fig. 9). The pores become slightly smaller as a result of immobilization of zirconocene dichloride (1–3 wt% Zr on the support), but the penetration of these molecules into the pores of MCM-41 can not be fully proved by these studies. The determination of the real internal pore size by thermoporometry could give more insight into the adsorption phenomenon.

Catalyst Activity in Ethene Polymerization

The preliminary ethene polymerization results show a clear difference in the catalyst activity of Grace silica (70°C), Si-MCM-41, and Al-modified MCM-41 (Si/Al = 32) supported metallocenes (Table 4). The molar ratio Al(MAO)/Zr was 2000. The blank reaction carried out in the same conditions using only MAO for the reaction did not show any activity. Taking the Zr content of the catalyst into consideration, the use of Si-MCM-41 as a support resulted in the lowest activity (6100 kgPE/(molZr · h); PE = polyethene), while the highest activity (15800 kgPE/(molZr · h)) was observed for the Al-modified MCM-41 (Si/Al = 32) supported metallocene. It could mean that the formation of inactive complexes between two metallocene molecules or between metallocene and methylaluminoxane was most successfully prevented in the latter case. The lower activity of the MCM-41 supported catalyst as compared

TABLE 3

The Results of N_2 Adsorption/Desorption and XRD Studies before and after the Immobilization of Cp_2ZrCl_2 (Pretreatment at 70°C)

Support/catalyst	BET surface area (m^2/g)	Pore volume (ml/g)	Average pore diameter (nm)	$Zr_{anal.}$ (wt%)	*d*-value, XRD (nm)
Grace SiO_2 (70°C)	372	1.70	6–25 nm (most 14 and 18 nm)		
Grace $SiO_2 + Cp_2ZrCl_2$	346	1.57	6–25 nm (most 14 and 18 nm)	1.2	
Si-MCM-41	1140	1.03	2.95		3.89
Si-MCM-41 + Cp_2ZrCl_2	1106	0.98	2.87	1.6	3.91
Si/Al = 32	1127	0.99	2.85		3.88
Si/Al = 32 + Cp_2ZrCl_2	917	0.64	2.64	2.7	3.99

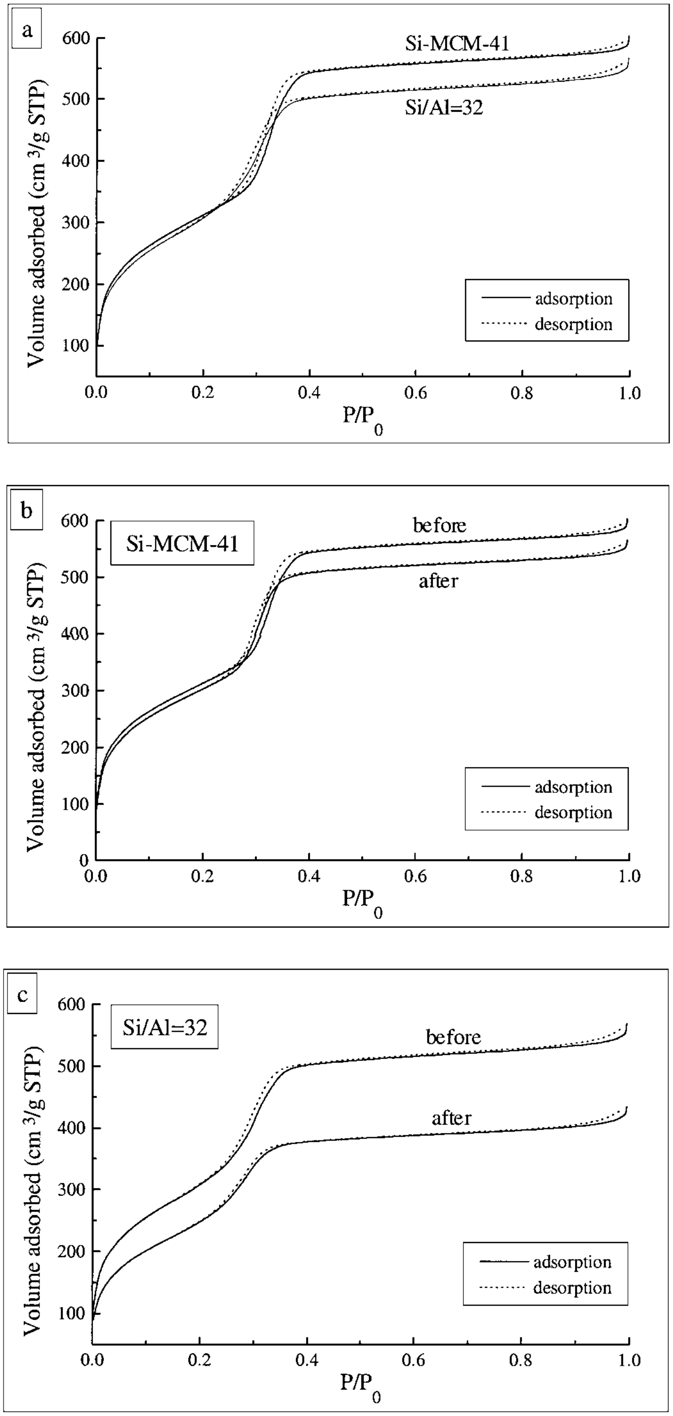

FIG. 9. The nitrogen adsorption/desorption isotherms (a) for Si-MCM-41 and Al-modified MCM-41, and (b) for Si-MCM-41, and (c) for Al-modified MCM-41 (Si/Al = 32) before and after the adsorption of Cp_2ZrCl_2.

to the Grace silica one could result from a steric hindrance in the pores of MCM-41. An activity of 29900 kgPE/(molZr · h) was obtained for homogeneous Cp_2ZrCl_2 under the same conditions.

The comparison of the observed activities with the literature values is rather difficult because of the different polymerization conditions used in every study. The activity values obtained in this study for homogeneous Cp_2ZrCl_2 are close to the values obtained in the literature, e.g., (46), 34000 kgPE/(molZr · h) with an Al(MAO)/Zr ratio of 1500 although also much lower values have been achieved, e.g., (13), 660–2095 kgPE/(molZr · h) with an Al(MAO)/Zr ratio of 200–500. The activities of the studied supported catalysts are high compared to values obtained by other research groups using Cp_2ZrCl_2/SiO_2 catalysts, when the active component has been deposited directly on the support. Sacchi *et al.* (13) obtained activities 11–207 kgPE/(molZr · h) for a heterogeneous catalyst using an Al/Zr molar ratio of 200–500. By using Cp_2ZrCl_2/HY-zeolite catalyst (Al/Zr = 1500) as high as 17900 kgPE/(molZr · h) activity has been achieved (46). The MAO-pretreatment of the SiO_2 support has usually been observed to increase slightly the catalyst activity, e.g., (47), 940 kgPE/(molZr · h) with an Al(MAO)/Zr ratio of 1000 and, e.g., (4), 4700 kgPE/(molZr · h) with Al(MAO)/Zr ratio of 200.

The weight-average molecular weights and the numerical values of the ratio of weight- to number-average molecular weights ($M_\mathrm{w}/M_\mathrm{n}$) observed for MCM-41 and Grace silica supported catalysts were almost the same, 430000–450000 g/mol and 2.2–2.3, respectively (Table 4). The homogeneous Cp_2ZrCl_2 produced polyethene with molecular weights of 482000 and 476000 g/mol and M_w/M_m ratios of 2.7 and 2.5 (Table 4). The molecular weights for the supported catalysts are observed to be slightly lower than those of the homogeneous complex. Often the values in the literature are higher for supported catalysts compared to homogeneous system (13). For example, in the studies of Sacchi *et al.* (13) molecular weights of 260000–270000 and up to 450000 were obtained for homogeneous and heterogeneous systems, respectively (Al(MAO)/Zr = 300–500). The observed molecular weight distributions are narrow around 2.2, which is a typical value for polymers prepared with metallocene catalysts (2). In some studies (12), the use of supported catalysts has also been observed to lead to higher M_w/M_m (2–5) of PE. The observed melting temperatures, T_m, of the polymers between 135 and 138°C are high, indicating the formation of linear high-density polyethene (48).

The partial desorption of the zirconocenes, L_2ZrR_2 (L = cyclopentadienyl, indenyl; $R = CH_3$, C_2H_5, Cl), from the support when reacting with MAO have been observed in several studies (7, 13, 14, 49). The stage of desorption depends on the polymerization conditions applied. The test reactions for the solution part (toluene soluble part) of the suspension after reaction of the catalyst with MAO were not done in the present work. According to the literature and studies carried out for a similar catalyst using the same reactor, the desorption might be fairly notable also in the reactions studied here.

TABLE 4

The Preliminary Results of Ethene Polymerizations with Silica Supported Cp_2ZrCl_2 Catalysts

Catalyst	Zr (wt%)	m_{cat} (mg)	n(Zr) (μmol)	Al/Zr	t_p (min)	Yield (g)	Activity in kg PE/(mol Zr · h)	T_m (°C)	M_w (gmol^{-1})	M_w/M_n
Cp_2ZrCl_2–Grace SiO_2[a]	1.2	3.4	0.46	2000	30	2.3	10000	137.3	451000	2.2
Cp_2ZrCl_2–Si-MCM-41	1.6	2.4	0.43	2000	60	2.6	6100	135.5	431000	2.3
Cp_2ZrCl_2–Si/Al = 32	2.7	1.4	0.41	2000	30	6.4	15800	137.9	451000	2.2
Cp_2ZrCl_2[b]		0.1	0.3	2000	30	5.1	29900	137.5	476000	2.5

[a] Cp_2ZrCl_2 was immobilized at 70°C.

[b] Homogeneous catalyst.

CONCLUSIONS

The structures of Grace silica and mesoporous silicate, MCM-41, are different. The MCM-41 has regular and hexagonally ordered pores inside the particles. Grace silica is formed of around 70-μm particle aggregates with large pores between the aggregates. It has lower BET surface area and broader pore size distribution than MCM-41. The well-defined pores of MCM-41 provide stable sites for attachment of the active component.

Using aluminium isopropoxide as a metal source, a hexagonally ordered pore structure could be obtained as less than 2.4 wt% of aluminium (Si/Al = 32) was involved. No evidence for AlOHSi bonding could be obtained for this support as deduced by solid-state ^{1}H-MAS-NMR and FTIR studies. However, two peaks in the ^{27}Al-NMR spectrum obtained for the Si/Al = 10 support indicated that aluminium is partly 4-coordinated and partly 6-coordinated. The Si/Al = 32 support was chosen for further studies in catalyst preparation and in ethene polymerization. The most active component, zirconocene dichloride, could be adsorbed on this support, revealing the presence of more reactive surface sites for Cp_2ZrCl_2 attachment. The ^{13}C-CPMAS NMR studies showed that zirconocene dichloride is attached to the support surface.

The preliminary ethene polymerization results show that the additional aluminium incorporated in the MCM-41 support (Si/Al = 32) has a big effect on catalyst activity. Clearly higher activity was observed as compared to the purely siliceous MCM-41 supported catalyst. The high surface area of MCM-41 could not be proved to have a large effect on the ethene polymerization reaction compared to the lower surface area material, Grace silica. The observed molecular weights of 431000–451000 g/mol and the M_w/M_m ratio of around 2.2 are typical for polymers prepared with metallocene catalysts. The melting temperatures, around 135°C, indicate the formation of linear high-density polyethene.

Further research will concentrate on whether the adsorption of an active component occurs in the pores. In order to diminish the desorption of an active component from a support, MAO could be adsorbed on the support before addition of Cp_2ZrCl_2. Also the activity of the studied catalysts in propene polymerization is of interest, where the structural effect might be important. Then the possibility of improving the tacticity of the polypropene is of special interest.

ACKNOWLEDGMENTS

Professor R. K. Harris from the Department of Chemistry, University of Durham, Great Britain, and Professor M. Hudson from the Department of Chemistry, University of Reading, Great Britain, are gratefully acknowledged for their collaboration. Dr. Andrew Root from Neste Company is thanked for solid-state ^{1}H-NMR measurements. The Academy of Finland and EU project ERB-FMRX CT96-0084 are acknowledged for financial support.

REFERENCES

1. Brintzinger, H. H., Fischer, D., Mühlhaupt, R., Rieger, B., and Waymouth, R. M., *Angew. Chem.* **34**, 1143 (1995).
2. Fink, G., Mülhaupt, R., and Brintzinger, H. H., "Ziegler Catalyst." Springer-Verlag, Berlin, 1995.
3. Repo, T., Klinga, M., Mutikainen, I., Su, Y., Leskelä, M., and Polamo, M., *Acta Chem. Scand.* **50**, 1116 (1996).
4. Janiak, C., and Rieger, B., *Die Angew. Macromol. Chem.* **215**, 47 (1994).
5. Soga, K., and Kaminaka, M., *Makromol. Chem. Phys.* **195**, 1369 (1994).
6. Collins, S., Kelly, W. M., and Holden, D. A., *Macromolecules* **25**, 1780 (1992).
7. Chien, J. C., and Dawei, H. J., *Polym. Sci. Part A* **29**, 1603 (1991).
8. Soga, K., Kim, H., and Shiono, T., *Makromol. Chem. Phys.* **195**, 3341 (1994).
9. Soga, K., Uozumi, T., Arai, T., Ban, H. T., and Kaji, E., *in* "Metcon '97: Polymers in Transition, June 4–5, Houston," 1997.
10. Ribeiro, M. R., Deffieux, A., and Portela, M. F., *Ind. Eng. Chem. Res.* **36**, 1224 (1997).
11. Richardson, J. T., "Principles of Catalyst Development," p. 26. Plenum, New York, 1989.
12. Burkhardt, T. J., Brinen, J. L., Hlatky, G. G., Spaleck, W. S., and Winter, A., World Patent 94 28034, 1994.
13. Sacchi, M. C., Zucchi, D., Tritto, J., Locatelli, P., and Dall'Occo, T., *Macromol. Rapid Commun.* **16**, 581 (1995).
14. Semikolenova, N. V., and Zakharov, V. A., *Macromol. Chem. Phys.* **198**, 2889 (1997).
15. Ciardelli, F., Altomare, A., and Michelotti, M., *Catal. Today* **41**, 149 (1998).
16. Lee, D.-H., and Yoon, K.-B., *Macromol. Rapid Commun.* **18**, 427 (1997).

17. Britcher, L., Eklund, T., Mikkola, P., Hakala, K., and Rosenholm, J. B., to be published.
18. Beck, J. S., Vartuli, J. C., Roth, W. J., Leonowicz, M. E., Kresge, C. T., Schmitt, K. D., Chu, C. T.- W., Olson, D. H., Sheppard, E. W., McCullen, S. B., Higgins, J. B., and Schlenker, J. L., *J. Am. Chem. Soc.* **114**, 10843 (1992).
19. Kresge, C. T., Leonowicz, M. E., Roth, W. J., Vartuli, J. C., and Beck, J. S., *Nature* **359**, 710 (1992).
20. Ko, Y. S., Han, T. K., Park, J. W., and Woo, S. I., *Macromol. Rapid Commun.* **17**, 749 (1996).
21. Woo, S. K., Ko, Y. S., Han, T. K., and Park, J. W., *in* "Metallocenes '96," pp. 271–292.
22. Van Loovren, L. K., Geysen, D. F., Vercruysse, K. A., Wouters, B. H., Grobet, P. J., and Jacobs, P. A., *Angew. Chem. Int. Ed.* **37**, 517 (1998).
23. Corma, A., *Chem. Rev.* **97**, 62373 (1997).
24. Linden, M., Schacht, S., Schuth, F., Steel, A., and Unger, K., *J. Porous Mater.* **5**, 177 (1998).
25. Corma, A., *J. Phys. Chem.* **99**, 1023 (1995).
26. Kytökivi, A., Ph.D. thesis, Helsinki University of Technology, Espoo, Finland, 1997. [55 pp.]
27. Zhao, X. S., Lu, G. Q., Whittaker, A. K., Millar, G. J., and Zhu, H. Y., *J. Phys. Chem. B* **101**, 6525 (1997).
28. Brun, M., Lallemand, A., Quinson, J.-F., and Eyraud, C., *Thermochim. Acta* **21**, 59 (1977).
29. Kloetstra, K. R., Zandbergen, H. W., van Koten, M. A., and van Bekkum, H., *Catal. Lett.* **33**, 145 (1995).
30. Cheng, C.-F., He, H., Zhou, W., Klinowski, J., Concalves, J. S., and Gladden, L. F., *J. Phys. Chem.* **100**, 390 (1996).
31. Webb, P. A., and Orr, C., "Analytical Methods in Fine Particle Technology." Micromeritics Instrument Corp. Norcross, 1997.
32. Romero, A. A., Alba, M. D., and Klinowski, J., *J. Phys. Chem. B* **102**, 123 (1998).
33. Luan, Z., Cheng, C.-F., He, H., and Klinowski, J., *J. Phys. Chem.* **99**, 10590 (1995).
34. Corma, A., *J. Catal.* **148**, 569 (1994).
35. Busio, M., Jänchen, J., and van Hooff, J. H. C., *Microporous Mater.* **5**, 211 (1995).
36. Reddy, K. M., and Song, C., *Catal. Lett.* **36**, 103 (1996).
37. Kosmas, M., Kolonia, K., Bokaris, E., Keene, M., Rouquerol, J., Pomonis, P., Denoyel, R., and Llewellyn, P., submitted for publication.
38. Brun, M., Quinson, J. F., and Eyraud, C., *L'actualité Chim.* **X**, 21 (1979).
39. Janicke, M. T., Landry, C. C., Christiansen, S. C., Kumar, D., Stucky, G. D., and Chmelka, B. F., *J. Am. Chem. Soc.* **120**, 6940 (1998).
40. Haukka, S., Ph.D. Thesis, University of Helsinki, Helsinki, 1993. [46 pp.]
41. Jentys, A., Pham, N. H., and Vinek, H., *J. Chem. Soc., Faraday Trans.* **92**, 3287 (1996).
42. Rahiala, H., Puputti, J., Beurroies, I., Stathopoulos, V., and Rosenholm, J. B., to be published.
43. Iiskola, E. I., Timonen, S., Pakkanen, T., Härkki, O., Lehmus, P., and Seppälä, J. V., *Macromolecules* **30**, 2853 (1997).
44. Kröger-Laukkanen, M., Peussa, M., Leskelä, M., and Niinistö, L., to be published.
45. Maschmeier, T., Rey, F., Sankar, G., and Thomas, J. M., *Nature* **378**, 159 (1995).
46. Ciardelli, F., Altomare, A., Arribas, G., and Conti, G., "Catalyst Design for Tailor-Made Polyolefins," p. 257. Kodansha, Tokyo, 1994.
47. Lee, D.-H., and Yoon, K.-B., *Macromol. Symp.* **97**, 185 (1995).
48. Billmeyer, F. W., Jr., "Textbook of Polymer Science," pp. 332, 366. Wiley, New York, 1984.
49. Soga, K., and Kaminaka, H., *Macromol. Chem. Rapid. Commun.* **13**, 221 (1992).